МІНІСТЕРСТВО ОСВІТИ ТА НАУКИ УКРАЇНИ
НАЦІОНАЛЬНИЙ АВІАЦІЙНИЙ УНІВЕРСИТЕТ
КАФЕДРА КОНСТРУКЦІЇ ЛІТАЛЬНИХ АПАРАТІВ

ДОПУСТИТИ ДО ЗАХИСТУ
Завідувач кафедри
д.т.н., професор.
___________ С.Р. Ігнатович
«___» __________ 2021 р.

ДИПЛОМНА РОБОТА

ВИПУСКНИКА ОСВІТНЬОГО СТУПЕНЯ БАКАЛАВРА

ЗІ СПЕЦІАЛЬНОСТІ
«АВІАЦІЙНА ТА РАКЕТНО-КОСМІЧНА ТЕХНІКА»

Тема: «Аванпроект середньомагістрального пасажирського літака місткістю до 150 пасажирів»

Виконавець: ___________ **Вань Цзян'нань**

Керівник: к.т.н., доцент ___________ **В.С. Краснопольський**

Нормоконтролер: к.т.н., доцент ___________ **С.В. Хижняк**

Київ 2021

MINISTRY OF EDUCATION AND SCIENCE OF UKRAINE

NATIONAL AVIATION UNIVERSITY

DEPARTMENT OF AIRCRAFT DESIGN

APPROVED BY
Head of department
D.Sc., professor
__________ S.R. Ignatovych
«___» _________ 2021.

BACHELOR THESIS

ON SPECIALITY
"AVIATION AND SPACE ROCKET TECHNOLOGY"

Topic: «Preliminary design of the mid-range passenger aircraft with 150 passenger capacity»

Prepared by: __________ **Wan Jiangnan**

Supervisor: PhD, associate professor __________ **V.S. Krasnopolskii**

Standard controller: PhD, associate professor __________ **S.V. Khyzhnyak**

Kyiv 2021

НАЦІОНАЛЬНИЙ АВІАЦІЙНИЙ УНІВЕРСИТЕТ

Факультет аерокосмічний

Кафедра конструкції літальних апаратів

Освітньо-кваліфікаційний ступінь «Бакалавр»

Спеціальність 134 «Авіаційна та ракетно-космічна техніка»

Освітня програма «Обладнання повітряних суден»

ДОПУСТИТИ ДО ЗАХИСТУ
Завідувач кафедри
д.т.н., професор.
_______________ С.Р. Ігнатович
«___» ___________ 2021 р.

ЗАВДАННЯ
на виконання дипломної роботи студента
Вань Цзянь'нань

1. Тема роботи: «Аванпроект середньомагістрального пасажирського літака місткістю до 150 пасажирів», затверджена наказом ректора від 21 травня 2021 року №815/ст.

2. Термін виконання проекту: з 24 травня 2021 р. по 20 червня 2021 р.

3. Вихідні дані до проекту: крейсерська швидкість V_{cr} = 824 км/год, дальність польоту L = 5000 км, крейсерська висота польоту H_{op} = 11,27 km.

4. Зміст пояснювальної записки: вступ, основна частина, що включає аналіз літаків-прототипів і короткий опис проектованого літака, обґрунтування вихідних даних для розрахунку, розрахунок основних льотно-технічних та геометричних параметрів літака, компонування пасажирської кабіни, розрахунок центрування літака, спеціальна частина, яка містить проект сидіння для крісла пілота.

5. Перелік обов'язкового графічного матеріалу: загальний вигляд літака (А1×1), компонувальне креслення фюзеляжу (А1×1), проект сидіння крісла пілота (А1×1).

6. Календарний план-графік

№ пор.	Завдання	Термін виконання	Відмітка про виконання
1	Отримання завдання, обробка статистичних даних.	24.05.2021-30.05.2021	
2	Розрахунок мас літака та його основних льотно-технічних характеристик.	31.05.2021-02.06.2021	

3	Розрахунок центрування літака.	03.06.2021-04.06.2021	
4	Розробка креслень по основній частині.	05.06.2021-06.06.2021	
5	Проектування сидіння крісла пілота та розробка креслень по спеціальній частині.	07.06.2021-11.06.2021	
6	Оформлення пояснювальної записки.	12.06.2021-13.06.2021	
7	Захист дипломної роботи	14.06.2021-20.06.2021	

7. Дата видачі завдання: «24» травня 2021 року.

Керівник дипломної роботи ____________ В.С. Краснопольський
(підпис керівника) П.І.Б.

Завдання прийняв до виконання ____________ Вань Цзянь'нань
(підпис студента) П.І.Б.

NATIONAL AVIATION UNIVERSITY

Faculty ____Aerospace______
Department __of Aircraft Design__
Educational degree __«Bachelor»__
Specialty 134 "Aviation and space rocket technology"
Educational program __"Aircraft equipment"__

APPROVED BY
Head of department
D.Sc., professor
___________ S.R. Ignatovych
«___» _________ 2021.

TASK
for the bachelor thesis
Wan Jiangnan

1. Topic: «Preliminary design of the mid-range passenger aircraft with 150 passenger capacity» approved by the Rector's order №815/ст. «21» May 2021 year.
2. Thesis terms: since 24.05.2021 year till 20.06.2021 year.
3. Initial data: cruise speed V_{cr} = 824 km/h, flight range L = 5000 km, operating altitude H_{op} = 11.27 km.
4. Content: introduction; main part: analysis of prototypes and brief description of designing aircraft, selection of initial data, wing geometry calculation and aircraft layout, landing gear design, engine selection, center of gravity calculation, special part: introduction and calculation of the pilot's seat.
5. Required material: general view of the airplane (A1×1), layout of the airplane (A1×1), pilot's seat design (A1×1).
6. Thesis schedule

№	Task	Time limits	Done
1	Task receiving, processing of statistical data.	24.05.2021-30.05.2021	
2	Aircraft take-off mass determination and flight performances calculation.	31.05.2021-02.06.2021	
3	Aircraft centering determination.	03.06.2021-04.06.2021	
4	Graphical design of the aircraft and its layout.	05.06.2021-06.06.2021	
5	Design of pilot's seat and calculations. Drawings of the special part.	07.06.2021-11.06.2021	
6	Completion of the explanation note.	12.06.2021-13.06.2021	

7	Preliminary examination and defense of the diploma work.	14.06.2021-20.06.2021	

7. Date: «24» May 2021 year.

Supervisor _____________ V.S. Krasnopolskii

Student _____________ Wan Jiangnan

РЕФЕРАТ

Дипломна робота «Аванпроект середньомагістрального пасажирського літака місткістю до 150 пасажирів» містить:

52 сторінки, 4 рисунки, 6 таблиць, 13 літературних посилань

Об’єкт дослідження: процес проектування літака транспортної категорії.

Предмет дослідження: аванпроект середньомагістрального пасажирського літака місткістю до 150 пасажирів.

Мета роботи: створити аванпроект середньомагістрального пасажирського літака та визначити його основні льотно-технічні характеристики.

Методи дослідження: в роботі застосовано метод порівняльного аналізу літаків-прототипів для вибору найбільш обґрунтованих технічних рішень, а також методи інженерних розрахунків для отримання основних параметрів проектованого літака. В спеціальній частині застосовано аналіз напружено-деформованого стану для розрахунку на міцність елементів крісла пілота.

Наукова новизна результатів: в спеціальній частині обґрунтовано застосування нового сидіння в кріслі пілота, що підвищує комфорт, зменшує стомлюваність та має покращені вагові характеристики.

Практична цінність роботи: результати роботи можуть бути використані в авіаційній галузі та в навчальному процесі авіаційних спеціальностей.

ПАСАЖИРСЬКИЙ ЛІТАК, АВАНПРОЕКТ ЛІТАКА, ЦЕНТРУВАННЯ ЛІТАКА, КОМПОНУВАННЯ ПАСАЖИРСЬКОЇ КАБІНИ, РОЗРАХУНОК НА МІЦНІСТЬ КРІСЛА

ABSTRACT

Bachelor thesis «Preliminary design of a mid-range passenger aircraft with 150 passenger capacity»

52 pages, 4 figures, 6 tables, 13 references

Object of study – design process of a civil airplane.

Subject of study – is preliminary design of a mid-range passenger aircraft with 150 passenger capacity.

Aim of bachelor thesis – is to create a preliminary design of an airplane and estimate its flight performances.

Research and development methods – the design methodology is based on prototype analysis to select the most advanced technical decisions and engineering calculations to get the technical data of designed aircraft. In special part the stress-strain analysis is used to estimate stress state of pilot's seat.

Novelty of the results – is a new pilot seat cushion that increases comfort and reduce tiredness.

Practical value – the results of the work can be used in the aviation industry and in the educational process of aviation specialties.

PASSENGER AIRCRAFT, PRELIMINARY DESIGN, CENTER OF GRAVITY CALCULATION, PASSENGER CABIN LAYOUT, CALCULATION OF SEAT STRENGTH

Format	№	Designation	Name	Quantity	Notes
			<u>General documents</u>		
A4	1	NAU 21 08W 00 00 00 28 TW	Task for work	1	
	2	NAU 21 08W 00 00 00 28	Mid-range passenger aircraft	2	
A1		Sheet 1	General view		
A1		Sheet 2	Fuselage layout		
A4	3	NAU 21 08W 00 00 00 28 EN	Mid-range passenger aircraft	52	
			Explanatory note		
			<u>Documentation for assembly units</u>		
A1	4	NAU 21 08W 00 00 00 28	Design of pilot’s seat	1	

		NAU 21.08W.00.00.00.28 EN				
Done by	Wan Jiangnan	Preliminary design of mid-range passenger aircraft with 150 passenger capacity (List of diploma work)	list	sheet	sheets	
Supervisor	Krasnopolskii V.S.			9	52	
			ASF 402			
St.control.	Khyzhniak S.V.					
Head of dep.	Ignatovich S.R.					

CONTENT

INTRODUCTION

Airplane is currently the fastest means of transportation, but because of his expensive air tickets, it has not yet been accepted by everyone. Compared with other means of transportation, airplanes have many advantages: high speed, safe and comfort. According to the statistics of the International Civil Aviation Organization, the average death toll per 100 million passenger-kilometers in civil aviation is 0.04, which is one-tenth to one-hundredth of the death toll from ordinary traffic accidents. It is a safer transportation method than a train. But airplanes as a means of transportation also have their own disadvantages as tickets price. Both the airplane itself and the fuel consumed during the flight have much higher cost than other modes of transportation.

Therefore, we should reduce the flight cost of the aircraft and the cost of aircraft manufacturing during its design. In order to meet the standards of comfort on short and medium range airlines we should also consider the comfort of the aircraft.

The goal of this project is to design an aircraft capable to transport 150 passengers and luggage over long distances and improve the comfort of the pilot's seat by introducing the new cushion with shape memory effect.

1. PROJECT PART. PRELIMINARY DESIGN OF MID RANGE AIRCRAFT

1.1 Analysis of prototypes and short description of designed aircraft

The overall design of the aircraft is the process of learning the design requirements, transforming the design parameters and determining the general view of the aircraft. The airplane design parameters are the design variables that determine the aircraft's flight performances. To determine a general view a set of design parameters needs to be determined including the mass of the aircraft and its various components, as well as geometrical parameters and engine performances.

At the initial stage of the design, it is very difficult to select all the parameters at once and it is often necessary to make a rough preliminary selection using statistical analysis. This analysis is based on the experience and decisions of the designers for similar aircrafts. If the designed aircraft is the successor of a certain active one and the performance index is not very different or there is only a large difference in two points, the original aircraft can be used as the prototype. The prototype for the designed aircraft in this work is A320-200. Statistic data of prototypes are presented in table 1.1.

Table 1.1

Performances of prototype – A320-200

Parameter	**Value**
The purpose of airplane	Passenger
Crew/flight attend. persons	2/5
Maximum take-off weight, m_{tow}, kg	73000
Maximum payload, $m_{k.max}$, kg	18260
Passenger's seat	150
The flight altitude, $V_{w.ex.}$, m	11270
Range, $m_{k.max}$, km	5000
Take-off distance, $L_{t.d.}$, m	2058
Number and type of engines	2xCFM56
Aspect Ratio	9,39
Taper Ratio	4.1
Sweepback angle at 1/4 chord line, ^{0}	28

1.2 Brief description of the main parts of the aircraft

1.2.1 Wing

The wing of the airplane has cantilever type with a supercritical rear-loaded airfoil. In order to adapt to the characteristics to short and average flight distances the design cruising speed is reduced to M 0.76-0.78. It is required because the wing characteristics change little with the cruising speed and the aerodynamic drag is low in entire range of use. The thickness of the rear beam of the airfoil has been increased by 30% to allow sufficient space for the flaps and their control system. Using "wingtip sails", the leading edge is round, the trailing edge is wedge-shaped, and there is a "spindle" extending backward along the chord of the wing to suppress induced drag. Compared with the "winglet", this device still has a better drag reduction effect in the non-designed state. When the crosswind enters the field, the "wingtip sail" itself will not stall. The full wingspan leading edge slat is divided into five sections. Because the engine nacelle is located close to the lower surface of the wing the engine pendant has been partially modified without compromising the high-speed cruise performance to improve the spread of the leading edge slat opening position. Both the inner and outer trailing edge flaps has large single-slot Fowler flaps. There are 5 spoilers on the upper surface of each side of the wing. Two on the inner side are used as speed brakes, three on the outer side for roll control, and all five are used for reducing lift force during landing. The inboard ailerons have been eliminated, which can improve the spanwise length of the trailing edge flaps during take-off and landing and increase the lift effect. The front and rear edges of each wing are fixed panels, trailing edge flaps, flap fairings, spoilers, ailerons and wing root fairings are made of composite materials.

1.2.2 Fuselage

The fuselage has semi-monocoque structure. The equal-diameter section of the fuselage is the longest and contain passenger cabin. In order to reduce resistance, a waist-shaped rear fuselage section is adopted. The structure consists of set of frames, stringers, beams and working skin.

1.2.3 Tail unit

Tail unit consists of the horizontal and vertical stabilizers, elevators and rudder The tail unit has a conventional configuration, the horizontal tail made with reverse camber to improve flight stability, the elevator is operated by fly-by-wire control system and the rudder by hydromachenical flight control system. Horizontal and vertical stabilizers have full-composite structure.

1.2.4 Landing gear

The landing gear includes two retractable main landing gear and one nose retractable landing gear. All landing gear struts and their hatches are hydraulically and electrically controlled. The hatch connected with the landing gear struts is driven by the landing gear mechanically: when landing gear is fully retracted – hatch is closed. During the retracting and expanding of the landing gear all landing gear hatches are opened.

The landing gear is retracted hydraulically. Each landing gear is a two-wheeled strut with oil-gas shock absorbers. The wing-fuselage fairing houses the main landing gear. The nose gear can be turned and moved forward into the fuselage. The main landing gear hatch is made of composite materials.

1.2.5 Control system

The entire flight process from take-off to landing is controlled by the fly-by-wire control system. The main fly-by-wire control system has two independent systems with five computers in total. Two are used for elevator and aileron control and three are used for spoiler control. The rudder trim is completed by two flight stabilization computers, and the control of the slat and flaps is performed by two special computers. All use fly-by-wire control, which not only improves flight safety, but also greatly reduces the load to the pilot. In order to improve the reliability of the fly-by-wire control system two measures have been taken: the signal transmission cables leading to each control surface are separated from each other, such as the aileron and spoiler cables are respectively laid before and after the wing front beam: In order to prevent lightning strikes, all telex control cables are installed in metal shielding sleeves and their exposed parts are sleeved in cable ducts. This type of flight control system uses side sticks instead of ordinary steering sticks and hand wheels. This side stick control system reduces the weight of the entire system. The side stick control system includes a joystick that tilts inward and forward, a roll and pitch sensor box and an artificial sensor system. When using the autopilot, a bayonet driven by an electromagnetic coil locks the control system in a neutral position. The electronic circuit is connected between the two fly-by-wire control devices. Under normal circumstances two pilots cannot operate the aircraft at the same time. In order to solve the contradiction of the inconsistent control input of the two pilots a comparison device is installed in the electronic circuit. The fly-by-wire control system can superimpose the two input signals. If one pilot wants to cancel the input of the other just press and hold the "takeover button" to release the other party's manipulation input. The hydraulic systems are color-coded in three groups: green, yellow and blue. The green and yellow systems are interconnected and each engine drives one. The blue hydraulic system driven by air ram wheels is equipped with three engines two of which are driven by engines for normal power supply and the other engine is driven by auxiliary power unit. It can also be utilized as an emergency backup in the air power supply, in addition to ground use. In the event of failure of all three engines, there is also a 5,000 VA emergency engine driven by a blue hydraulic system a converter is also installed to provide DC power, and a battery is also provided.

1.2.6 Onboard equipment

Two-person "glass" cockpit is equipped by controls of all the aircraft systems located on the top panel. The display system belongs to the second generation, which consists of three display management computers and two system data acquisition devices. It adopts the second-generation digital automatic flight system integrated with the fly-by-wire control system. Therefore, there is no special guidance computer and engine thrust control computer on the aircraft and there is no independent servo mechanism for autopilot and auto throttle. These functions are all included in the flight management computer. The command signal of the computer is provided to the pitch through the fly-by-wire control computer and the roll control surface is controlled by the flight stabilization computer to control the yaw. Thrust control is part of the engine's full-function electronic control system. There are only six computers for such automatic flight control systems. The second-generation digital automatic flight system with a higher degree of comprehensiveness is adopted which improves safety and reliability, simplifies the system and reduces the cost and weight of the aircraft. A centralized fault display system is adopted. When the aircraft system fails, the two cathode-ray tubes in the center of the instrument panel respectively display warning signals and system movement. The controller and display device automatically analyze the cause of the failure through the integrated failure display system to avoid unnecessary reading of manuals and documents.

Each cabin crew member place is equipped with a communication system, including a telephone and a flight attendant panel. The cabin door has a single-channel evacuation slide which is equipped with a lighting system. Oxygen masks are located above the passengers and each cabin crew member including some other emergency equipment.

1.2.7 Choice and description of power plant

The engines of these series are all CFM56-2. The main performances are similar and they can be used in the designed aircraft. For this project was chosen CFM56-2C1 according its take-off thrust that is obtained from the calculation. The data of these engines are presented in table 1.2.

Table 1.2

Engines performances

Model	Thrust	Bypass ratio	Dry weight
CFM56-2A-2	24,000 lbf (110 kN)	5.9	4,820 lb (2,190 kg)
CFM56-2B1	22,000 lbf (98 kN)	6.0	4,671 lb (2,120 kg)
CFM56-2C1	22,000 lbf (98 kN)	6.0	4,635 lb (2,100 kg)

1.3 Geometry calculations for the main parts of the aircraft

Layout of the aircraft is determined by relative disposition of its parts and structures and requires the calculation of all types of loads caused by passengers, cargo, fuel and so on. The choice of the scheme, composition and aircraft parameters is directed to the best meets the operational requirements.

1.3.1 Wing geometry calculation

Geometrical characteristics of the wing are determined from the take-off weight m_0 and specific wing load p_0.

Full wing area with extensions is:

$$S_w = \frac{m_0 \cdot g}{p_0} = \frac{71894 \cdot 9.8}{4987} = 141.28\ \mathrm{m}^2,$$

where S_w – wing area, m^2; g – acceleration due to gravity m/s^2.

Relative wing extensions area is 0.01.

Wing span is:

$$l = \sqrt{S_w \cdot \lambda_w} = \sqrt{141.28 \cdot 9.39} = 36.4\ \mathrm{m},$$

where l – wing span, m; λ_w – wing aspect ratio.

Root chord is:

$$b_0 = \frac{2S_w \cdot \eta_w}{(1+\eta_w) \cdot l} = \frac{2 \cdot 141.28 \cdot 4.1}{(1+4.1) \cdot 36.4} = 6.24\ \mathrm{m},$$

where b_0 – root chord, m; η_w – wing taper ratio.

Tip chord is:

$$b_t = \frac{b_0}{\eta_w} = \frac{6.24}{4.1} = 1.52\ \mathrm{m},$$

where b_t – tip chord, m.

Maximum wing thickness is determined in the forehead i-section and is equal to:

$$c_i = c_w \cdot b_t = 0.12 \cdot 1.52 = 0.1824 \text{ m},$$

where c_i – wing thickness in i-section, m; c_w – related wing thickness.

On board chord for trapezoidal shaped wing is:

$$b_b = b_0 \cdot \left(1 - \frac{(\eta_w - 1) \cdot D_f}{\eta_w \cdot l_w}\right) = 6.24 \cdot \left(1 - \frac{(4.1 - 1) \cdot 3.7}{4.1 \cdot 36.4}\right) = 5.76 \text{ m},$$

where b_b – wing board chord, m; D_f – fuselage diameter, m.

Type of wing structural scheme determines quantity of spars and its position as well as places of wing joints.

On the modern aircraft usually used double or triple spar wing. The designed aircraft has two spars.

The geometrical method was used for mean aerodynamic chord determination (fig. 1.1). Mean aerodynamic chord is equal to b_{MAC} = 4.3512 m.

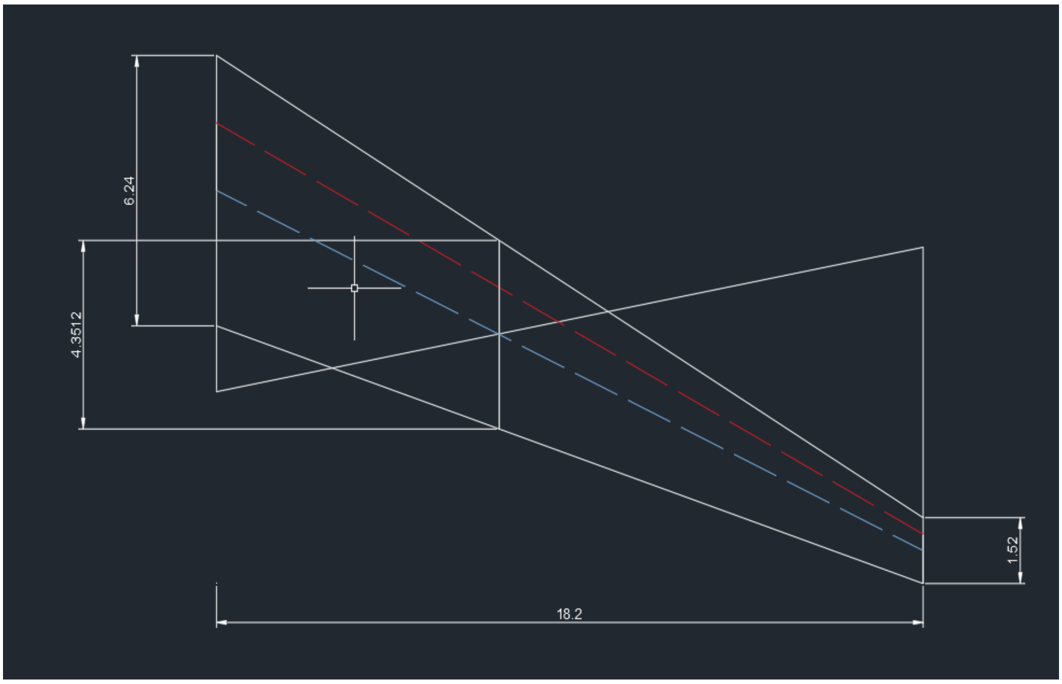

Fig. 1.1. Determination of mean aerodynamic chord.

After the determination of the geometrical characteristics of the wing it is possible to estimate ailerons and high-lift devices geometry.

Ailerons geometrical parameters are determined in next consequence:

Ailerons span is:

$$l_{ail} = 0.35 \cdot \frac{l}{2} = 0.35 \cdot \frac{36.4}{2} = 6.37 \text{ m},$$

where l_{ail} – ailerons span, m.

Aileron area is:

$$S_{ail} = 0.07 \cdot \frac{S_w}{2} = 0.07 \cdot \frac{141.28}{2} = 4.95 \text{ m}^2,$$

where S_{ail} – ailerons area, m.

Increasing of l_{ail} and b_{ail} more than recommended values is not necessary and convenient. With the increase of l_{ail} more than given value the increase of the ailerons coefficient falls, and the high-lift devices span decreases. With b_{ail} increase, the width of the wing chord decreases.

In the airplanes of the third generation there is a tendency to decrease relative wing span and ailerons area. In this case for the transversal control of the airplane we use spoilers together with the ailerons. Due to this the span and the area of high-lift devices may be increased that improves take-off and landing characteristics of the aircraft.

The aim of determination of wing high-lift devices geometrical parameters is the providing take-off and landing coefficients of wing lift force, assumed in the previous calculations with the chosen rate of high-lift devices and the type of the airfoil.

In the modern design the rate of the relative chords of wing high-lift devices is:

b_{sf} = 0.25…0.3 – for the split edge flaps;

b_f = 0.28…0.3 – one slotted and two slotted flaps;

b_f = 0.3…0.4 – for three slotted flaps and Fowler’s flaps;

b_s = 0.1…0.15 – slats.

Effectiveness of high-lift devices rises proportionally to the wing span increase, serviced by high-lift devices, so we need to obtain the biggest span of high lift devices due to use of flight spoiler and minimize the area of engine and landing gear nacelles.

To choose the structural scheme, hinge-fitting scheme and kinematics of the high-lift devices it is needed to take into account the statistics and experience of native and foreign aircraft designs. Have to be mentioned that in the majority of existing designs of high-lift devices they are made by spar structural scheme.

1.3.2 Fuselage layout

To choose the shape and the size of fuselage cross section it is needed to take into account aerodynamic demands. The shape of the fuselage influences on value of aerodynamic drag. Application of circular shape of fuselage nose part significantly minimize its drag. For transonic airplanes fuselage nose part has to be:

$$l_{fnp} = 1.5 \cdot D_f = 1.5 \cdot 3.7 = 5.55 \text{ m},$$

where D_f – fuselage diameter, m; l_{fnp} – length of fuselage nose part.

Except aerodynamic requirements it is necessary to consider the strength and layout requirements.

To provide minimal weight the best fuselage cross section shape is circular. In this case the fuselage has the minimal skin width. As the partial case may be used the combination of two or more vertical or horizontal series of circles.

To geometrical parameters used in calculation are: fuselage diameter D_f, fuselage length l_f, fuselage aspect ratio λ_f, fuselage nose part aspect ratio λ_{np}. Fuselage length is determined considering the aircraft scheme, layout and airplane center-of-gravity position peculiarities and landing angle of attack α_{land}.

Fuselage length is equal to:

$$l_f = \lambda_f \cdot D_f = 9.51 \cdot 3.7 = 35.187 \text{ m}.$$

Fuselage nose part aspect ratio is equal to:

$$\lambda_{fnp} = \frac{l_{fnp}}{D_f} = \frac{5.55}{3.7} = 1.5.$$

Length of the fuselage rear part is equal to:

$$l_{frp} = \lambda_{frp} \cdot D_f = 3.1 \cdot 3.7 = 11.47 \text{ m}.$$

During the determination of fuselage length it is necessary to get minimum mid-section on the one hand and meet layout demands on the other.

For passenger airplanes fuselage mid-section first of all depends on the size of passenger cabin. One of the main parameter that determines the mid-section of passenger airplane is the height of the passenger cabin.

Cabin height is equal to:

$$H_{cab} = 1.48 + 0.17 \cdot B_{cab} = 1.48 + 0.17 \cdot 3.6 = 2.014 \text{ m},$$

where H_{cab} – cabin height, m; B_{cab} – width of the cabin, m.

From the design point of view it is convenient to have round cross section, because in this case it'll be the strongest and the lightest. But for passenger and cargo placing this shape is not always the most convenient one. In the most cases one of the most suitable ways is to use the combination of two circles intersection or oval shape of the fuselage. But the oval shape is not suitable in the production, because the upper and lower panels will bend due to extra pressure and will demand extra bilge beams or rectangular with the rounded corners.

The width of the cabin in the economic class where seats are located in one row (3+3) is:

$$B_{cab} = n_3 b_3 + n_{aisle} \cdot b_{aisle} + 2\delta = 2 \cdot 1.34 + 2 \cdot 0.41 + 2 \cdot 0.05 = 3.6 \text{ m},$$

where n_3 – number of three-seat blocks; b_3 – width of three-seat blocks, m; n_{aisle} – number of aisles; b_{aisle} – width of aisle, m; δ – distance between external armrests to the decorative panels, m.

The length of passenger cabin is equal to:

$$L_{cab} = L_1 (n_{rows} - 1) \cdot L_{sp} + L_2 = 1.2 \cdot (25 - 1) \cdot 0.87 + 0.25 = 25.31 \text{ m},$$

where L_{cab} – length of passenger cabin, m; L_1 – distance from the wall to the back of the seat in first row, m; L_2 – distance from the back of the seat in last row to the wall, m; n_{rows} – number of rows; L_{sp} – seat pitch, m.

1.3.3 Luggage compartment

Given the fact that the unit load on floor K = 400…600 kg/m^2

The area of cargo compartment is:

$$S_{cargo} = \frac{M_{bag}}{0.4K} + \frac{M_{c\&m}}{0.6K} = \frac{3000}{0.4 \cdot 400} + \frac{900}{0.6 \cdot 600} = 22.5\,\text{m}^2,$$

where S_{cargo} – cargo compartment volume, m^3; M_{bag} – mass of the baggage, kg; $M_{c\&m}$ – mass of the cargo and mail, kg.

Cargo compartment volume is equal to:

$$\nu_{cargo} = \nu_c \cdot n_{pass} = 0.2 \cdot 150 = 30\,\text{m}^3,$$

where ν_{cargo} – cargo compartment volume, m^3; ν_c – cargo volume coefficient, m^3; n_{pass} – number of passengers. Luggage compartment design is similar to the prototype.

1.3.4 Galleys and buffets

International standards require two dishes for airplanes with mixed layout. Kitchen cupboards must be placed between the cockpit and passenger cabin. Refreshment and food can not be placed near the toilets and wardrobes. Volume of buffets and galleys is equal to:

$$v_{galley} = v_g \cdot n_{pass} = 0.1 \cdot 150 = 15\,\text{m}^3,$$

where ν_{galley} – galley volume, m^3; ν_g – galley volume coefficient, m^3; n_{pass} – number of passengers.

Area of buffets and galleys is equal to:

$$S_{galley} = \frac{\nu_{galley}}{H_{cab}} = \frac{15}{2.014} = 7.45\,\text{m}^2,$$

where S_{galley} – galley area, m^2.

Number of meals per passenger breakfast, lunch and dinner – 0,75 kg; tea and water – 0,45 kg. Passengers are fed every 3.5…4 hour of flight. Buffet design is similar to prototype.

1.3.5 Lavatories

Number of toilet facilities is determined by the number of passengers and flight duration: with t > 4:00 one toilet for 40 passengers. The number of lavatories is equal to:

$$n_{lav} = \frac{n_{pass}}{40} = \frac{150}{40} = 3.75$$

where n_{lav} – number of lavatories.

So the chosen number of lavatories is 4. Area of each lavatory is 1.6 m^2 and width – 1 m. Toilets design is similar to the prototype.

1.3.6 Layout and calculation of basic parameters of tail unit

One of the most important tasks of the aerodynamic layout is the choice of tail unit configuration. To provide longitudinal stability during flight its center of gravity should be placed in front of the aircraft focus and the distance between these points, related to the mean value of wing aerodynamic chord, determines the rate of longitudinal stability (1.1).

$$m_x^{C_y} = \overline{x_T} - \overline{x_F} < 0, \qquad (1.1)$$

where $m_x^{C_y}$ – is the moment coefficient; x_T, x_F – center of gravity and focus coordinates.

If $m_x^{C_y} = 0$ the plane has the neutral longitudinal static stability, if $m_x^{C_y} > 0$ the plane is statically instable. In the normal aircraft scheme (tail unit is behind the wing), focus of the combination wing-fuselage during the install of the tail unit moves back. Next step is determination of the tail unit geometrical parameters.

Area of vertical tail unit is equal to:

$$S_{VTU} = \frac{l_w \cdot S_w}{L_{VTU}} \cdot A_{VTU} = \frac{36.4 \cdot 141.28}{13.84} \cdot 0.08 = 29.73 \text{ m}^2,$$

where S_{VTU} – area of vertical tail unit, m^2; L_{VTU} – length of vertical tail unit, m; A_{VTU} – coefficient of static moment of vertical tail unit.

Area o horizontal tail unit is equal to:

$$S_{HTU} = \frac{b_{MAC} \cdot S_w}{L_{HTU}} \cdot A_{HTU} = \frac{4.3512 \cdot 141.28}{13.84} \cdot 0.8 = 35.52 \text{ m}^2,$$

where S_{HTU} – area of horizontal tail unit, m^2; L_{HTU} – length of horizontal tail unit, m; A_{HTU} – coefficient of static momentum of horizontal tail unit.

Values L_{HTU} and L_{VTU} depend on some factors. First of all their value are influenced by the length of he nose part and tail part of the fuselage, sweptback and wing location, and also from the conditions of stability and control of the airplane.

Altitude elevator area is:

$$S_{el} = k_{el} \cdot S_{HTU} = 0.35 \cdot 35.52 = 12.432 \text{ m}^2,$$

where S_{el} – elevator area, m^2; k_{el} – relative elevator area coefficient.

Rudder area is:

$$S_{rud} = k_r \cdot S_{VTU} = 0.4 \cdot 29.73 = 11.892 \text{ m}^2,$$

where S_{rud} – rudder area, m^2; k_r – relative rudder area coefficient.

Choose the area of aerodynamic balance:

$$0.3 \le M \le 0.6$$

$$S_{eb} = k_{eb} \cdot S_{el} = 0.22 \cdot 12.432 = 2.735 \text{ m}^2,$$

$$S_{rb} = k_{rb} \cdot S_{rud} = 0.2 \cdot 29.73 = 5.946 \text{ m}^2,$$

where S_{eb} – area of elevator aerodynamic balance, m^2; S_{rb} – area of rudder aerodynamic balance, m^2; k_{eb} – relative elevator balance area coefficient; k_{rb} – relative rudder balance area coefficient.

The area of altitude elevator trim tab is:

$$S_{te} = k_{te} \cdot S_{el} = 0.1 \cdot 12.432 = 1.2432 \text{ m}^2,$$

where S_{te} –elevator trim tab area, m^2; k_{te} – relative elevator trim tab area coefficient.

Area of rudder trim tab is:

$$S_{tr} = k_{tr} \cdot S_{rud} = 0.05 \cdot 11.892 = 0.5946 \text{ m}^2,$$

where S_{tr} –rudder trim tab area, m^2; k_{tr} – relative trim tab area coefficient.

Root chord of horizontal stabilizer is:

$$b_{0HTU} = \frac{2 \cdot S_{HTU} \cdot \eta_{HTU}}{(1+\eta_{HTU}) \cdot L_{HTU}} = \frac{2 \cdot 35.52 \cdot 2.15}{(1+2.15) \cdot 13.84} = 3.5 \text{ m},$$

where η_{HTU} – horizontal tail unit taper ratio; b_{0HTU} – root chord of horizontal stabilizer, m.

Tip chord of horizontal stabilizer is:

$$b_{tHTU} = \frac{b_{0HTU}}{\eta_{HTU}} = \frac{3.5}{2.15} = 1.63 \text{ m},$$

where b_{tHTU} – tip chord of horizontal stabilizer, m.

Root chord of vertical stabilizer is:

$$b_{0VTU} = \frac{2 \cdot S_{VTU} \cdot \eta_{VTU}}{(1+\eta_{VTU}) \cdot L_{VTU}} = \frac{2 \cdot 29.73 \cdot 4}{(1+4) \cdot 13.84} = 3.44 \text{ m},$$

where b_{0VTU} – root chord of vertical stabilizer, m; η_{VTU} – vertical tail unit taper ratio; L_{VTU} – vertical tail unit span.

Tip chord of vertical stabilizer is:

$$b_{tVTU} = \frac{b_{0VTU}}{\eta_{VTU}} = \frac{3.44}{4} = 0.86\ \text{m}.$$

where b_{tVTU} – tip chord of vertical stabilizer, m.

1.3.7 Landing gear design

To estimate the landing gear outline in this project it is necessary to calculate the location of every strut relatively to each other, to determine the loads on landing gear system, and its location considering centre of gravity of an airplane. In this layout the principal scheme of landing gear is fully based on the prototype data.

As in the case with the tail unit it is necessary to provide the aircraft with the stable and controllable base during operation on the ground including landing and take-off.

Main wheel axes offset is:

$$e = k_e \cdot b_{MAC} = 0.18 \cdot 4.3512 = 0.7832\ \text{m},$$

where k_e – coefficient of axes offset; e – main wheel axes offset, m.

With the large wheel axial offset the lift-off of the front gear during take of is complicated and with small the drop of the airplane on the tail is possible when the loading of the back of the airplane comes first.

Landing gear wheel base is:

$$B = k_b \cdot l_f = 0.35 \cdot 35.187 = 12.315\ \text{m},$$

where B – wheel base, m; k_b – wheel base calculation coefficient.

Front wheel axial offset is:

$$d_n = B - e = 12.315 - 0.7832 = 11.5318\ \text{m},$$

where d_n – nose wheel axes offset, m.

Wheel track is:

$$T = k_T \cdot B = 0.8 \cdot 11.5318 = 9.852\ \text{m},$$

where T – wheel track, m; k_T – wheel track calculation coefficient.

Wheels for the landing gear is chosen by the size and run loading on it from the take-off weight. For the front support it is necessary to consider dynamic loading as well.

Type of the pneumatics (balloon, half balloon, arched) and the pressure in it is determined by the runway surface, which should be used. There are breaks on the main wheel.

Nose wheel load is:

$$P_n = \frac{g \cdot e \cdot k_d \cdot m_0}{B \cdot z} = \frac{9.81 \cdot 0.7832 \cdot 1.75 \cdot 71894}{12.315 \cdot 2} = 39247 \text{ N},$$

where P_n – nose wheel load, N; k_d – dynamics coefficient; z – number of wheels.

Main wheel load is equal to:

$$P_m = \frac{9.81 \cdot (B - e) \cdot m_0}{B \cdot n \cdot z} = \frac{9.81 \cdot (12.315 - 0.7832) \cdot 71894}{12.315 \cdot 2 \cdot 4} = 51501 \text{ N},$$

where P_m – main wheel load, N; n – number of main landing gear struts.

According the calculated values of wheel loading and take-off speed it is possible choose the tires for landing gear from the catalog:

for nose landing gear

Aircraft Rib 461B-3434-TL with parameters $P_{rated} = 9000 \text{ lbf}$; $V_{rated} = 250 \text{ MPH}$; size 18×5.7-8.

for main landing gear

Aircraft Rib 461B-2728-TL with parameters $P_{rated} = 12000 \text{ lbf}$; $V_{rated} = 195\ MPH$; size 22×7.75-10.

The rate of wheel loading is:

for nose wheel $\frac{9000 - 8835}{9000} \cdot 100\% = 1.83\%$;

for main wheel $\frac{12000 - 11593}{12000} \cdot 100\% = 3.39\%$.

The values are less than 10% so choosed tires can be used for this airplane.

1.4 Center of gravity calculation

1.4.1 Trim-sheet of the equipped wing

Mass of the equipped wing contains the mass of its structure, mass of the equipment located in the wing and mass of the fuel. Regardless of the place of mounting (to the wing or to the fuselage) the main landing gear and the front gear are included in the mass register of the equipped wing. The mass register includes names of the objects, mass themselves and their center of gravity coordinates. The origin of the given coordinates of the mass centers is chosen by the projection of the nose point of the mean aerodynamic chord (MAC) for the surface XOY. The positive meanings of the coordinates of the mass centers are accepted for the aft part of the aircraft.

The list of the mass objects for the aircraft, where the engines are located under the wing, included the names given in the table 1.3. Coordinates of the center of mass for the equipped wing are defined by the formula (1.1).

$$X'_w = \frac{\sum m'_i \cdot x_i}{\sum m'_i}, \tag{1.1}$$

where X'_w – center of mass for equipped wing, m; m'_i – mass of a unit, kg; x_i – center of mass of the unit, m.

1.4.2 Trim-sheet of the equipped fuselage

Origin of the coordinates is chosen in the projection of the nose of the fuselage on the horizontal axis. For the axis X the construction part of the fuselage is given. The list of the objects for the equipped fuselage, with engines are mounted under the wing, is given in table 1.4. The CG coordinates of the equipped fuselage are determined by formula (1.2).

$$X'_f = \frac{\sum m'_i \cdot x_i}{\sum m'_i} \tag{1.2}$$

where X'_f – center of mass for equipped fuselage, m; m'_i – mass of a unit, kg; x_i – center of mass of the unit, m.

Table 1.3

Trim sheet of equipped wing

N	Name	Mass		CG coordinates x_i (m)	Moment $m_i x_i$ (kgm)
		Units	total mass m_i (kg)		
1	Wing (structure)	0.11492	8262.05848	1.95804	16177.44099
2	Fuel system	0.0075	539.205	1.95804	1055.784958
3	Airplane control, 30%	0.00195	140.1933	2.61072	366.0054522
4	Electrical equipment, 10%	0.00327	235.09338	0.43512	102.2938315
5	Anti-ice system, 50%	0.0115	826.781	0.43512	359.7489487
6	Hydraulic systems, 70%	0.01232	885.73408	2.61072	2312.403677
7	Power plant	0.07392	5314.40448	1	5314.40448
8	Equipped wing without landing gear and fuel	0.22538	16203.46972	1.614	25688.08233
9	Nose landing gear	0.004011	288.366834	-9.70428	-2798.3925
10	Main landing gear	0.036099	2595.301506	2.61072	6775.605548
11	Fuel	0.25837	18575.25278	1.95804	36371.08795
12	Equipped wing	0.52386	37662.39084	1.753377358	66036.38334

After the CG of fully equipped wing and fuselage is determined, the moment equilibrium equation (1.3) relatively to the fuselage nose can been made.

$$m_f X'_f + m_w (X_{MAC} + x'_w) = m_0 (X_{MAC} + C) \tag{1.3}$$

where m_0 – aircraft take-off mass, kg; m_f – mass of fully equipped fuselage, kg; m_w – mass of fully equipped wing, kg; C – distance from MAC leading edge to the CG point determined by the designer.

From here we determined the wing MAC leading edge position relative to fuselage, means X_{MAC} value by formula:

$$X_{MAC} = \frac{m_f \cdot X'_f + m_w \cdot X'_w - m_0 \cdot C}{m_0 - m_w} = \frac{34288 \cdot 16.62 + 37662 \cdot 1.75 - 71894 \cdot 0.32}{71894 - 37662} = 17.9\ \text{m}.$$

Table 1.4

Trim sheet of equipped fuselage

№	Objects	Mass		Coordinates of CG	Moment (kgm)
		Units	Total (kg)		
1	Fuselage	0.09735	6998.8809	17.5935	123134.8111
2	Horizontal tail	0.01112	799.46128	29	23184.37712
3	Vertical tail	0.01097	788.67718	29	22871.63822
4	Radar	0.0032	230.0608	0.5	115.0304
5	Radio equipment	0.0024	172.5456	1.2	207.05472
6	Instrument panel	0.0056	402.6064	1.3	523.38832
7	Navigation equipment	0.0048	345.0912	1.2	414.10944
8	Lavatory 1, 2, galley 1	0.00615	442.1481	4	1768.5924
9	Lavatory 3, 4, galley 2	0.00615	442.1481	28	12380.1468
10	Aircraft control system 70%	0.00455	327.1177	17.5935	5755.145255
11	Hydro-pneumatic system 30%	0.00528	379.60032	24.6309	9349.897522
12	Electrical equipment 90%	0.02943	2115.84042	17.5935	37225.03843
13	Nontypical equipment	0.0037	266.0078	15.834	4211.967505
14	Operational items	0.02149	1545.00206	2	3090.00412
15	Load devices equipment	0.0083	596.7202	15.834	9448.467647
16	Lining and insulation	0.0073	524.826	17.5935	9233.526231
17	Air-conditioning system, 25%	0.00575	413.39	17.5935	7272.976965
18	Anti-ice system 25%	0.00575	413.39	28.1496	11636.76314
19	Passenger seats (business)	0.000867	62.332098	6	373.992588
20	Passenger seats (economic class)	0.015383	1105.945402	18.4	20349.3954
21	Seats of flight attendance	0.000433	31.130102	7.5	233.475765
22	Seats of pilot	0.0002167	15.5794298	2.4	37.39063152
23	Additional equipment	0.0031	222.8714	15.834	3528.945748
24	**Equipped fuel without payload**	**0.2592897**	**18641.37249**	**16.43366848**	**306346.1355**
25	Passengers(business)	0.008464	608.510816	6	3651.064896
26	Onboard meal	0.00158	113.59252	4	454.37008
27	Baggage cargo, mail	0.051	3666.594	15.834	58056.8494
28	Crew	0.00635	456.5269	6	2739.1614
29	Passengers(economy)	0.150236	10801.06698	18.4	198739.6325
30	TOTAL	0.4769197	34287.66371	16.62368187	569987.2138

1.4.3 Calculation of center of gravity positioning variants

The list of mass objects for centre of gravity variant calculation given in table 1.5 and center of gravity calculation options given in table 1.6, completes on the base of both previous tables.

Table 1.5

Calculation of CG positioning variants

Name	Mass, kg	Coordinates CG, m	Moment, kgm
Object	m_i	x_i	M_i
Equipped wing (without fuel and landing gear)	16203.47	17.914	290268.9616
Nose landing gear (extended)	288.366834	6.59572	1901.986894
Main landing gear (extended)	2595.301506	18.91072	49079.0201
Fuel/fuel reserve	18575.25278	18.25804	339147.7083
Equipped fuselage (without payload)	18641.37249	16.43366848	306346.1355
Passengers of business class	608.5108	6	3651.0648
Passengers of economy class	10801.00698	18.4	198738.5284
Baggage cargo, mail	3666.594	15.834	58056.8494
Crew	235.09338	6	1410.56028
Nose landing gear	288.366834	5.81572	1677.060764
Main landing gear	2595.301506	19.13072	49649.98643
Reserve fuel	2302.76	19.5	44903.82

Table 1.6

Airplanes CG position variants

№	Variants of the loading	Mass, kg	Moment of the mass, kgm	Centre of the mass, m	Centering
1	Take-off mass (LG extended)	71894	1248600.815	17.36724644	0.245276346
2	Take-off mass (LG retracted)	71894	1248946.855	17.37205964	0.246382523
3	Landing weight (LG extended)	55342.47599	954356.927	17.24456504	0.217081505
4	Ferry version	56538.85699	988500.4128	17.48355848	0.272007373
5	Parking version	37728.51083	647596.1041	17.16463464	0.198711768

Conclusion to the project part

In this part the main geometric dimensions and centering of designed aircraft were determined. That made the creation of the drawing outline possible.

During the calculation the main geometrical parameters caused by operational purpose, planned quantities of passengers, speed and altitude of flight, conditions of landing and take-off were considered. All obtained values meet requirements for the short range passenger aircrafts.

The centering of the designed aircraft was performed. The most forward center of gravity position of equipped aircraft is 19.87 from the leading edge of main aerodynamic chord. The most aft center of gravity position of equipped aircraft is 27.2 from the leading edge of main aerodynamic chord. Between these values centering of the aircraft is provided.

Geometrical parameters almost match with chosen prototypes. That fact allows to make a conclusion that designed aircraft will successfully compete with another models on the chosen market segment.

Furthermore, the engine CFM56-2C1 that meets the requirements considering efficiency for designed aircraft was chosen. Main peculiarities of basic section of an aircraft and their influence on outline creation were figured out.

2. SPECIAL PART. THE NEW PILOT’S SEAT CUSHION

2.1 Introduction

Pilots and car drivers spend a significant amount of time on seats that are poorly designed and unpleasant. Furthermore, their postures could be unsuitable. Lower back pain, weariness and musculoskeletal diseases are consequences of this. As a result pilots' and drivers' seat comfort is an important problem. Recently, there has been a rising emphasis on good seat design with user pleasure in mind including comfort, safety, and performance. Seat comfort, on the other hand, is difficult to define and quantify. Pilots' incorrect postures when seated on seats that aren't well-designed create tiredness. When pilots worked in cockpit with little leg room the problem was exacerbated. The application of anthropometric parameters and biomechanical evaluations would help to prevent tiredness.

Commercial pilots' jobs in the airline business required them to work unusual hours and be extremely vigilant. However, a pilot's discomfort at work causes them to be less aware while flight. The performance of a pilot's seat is determined by a variety of elements, including seat dimensions, sitting positions, physical conditions and the possibility to reach every section of the control panel without strain. Tall pilots stub their legs on the control panel during take-off and landing, according to a research conducted on the Boeing 747 pilot seat. According to this study, the 95th percentile of height found the workstation of this aircraft to be unpleasant. However, the majority of pilots have experienced similar physical effects and accept it as part of their profession.

Pilots who sit for long periods of time experience back pain, tingling, and discomfort in their buttocks, legs and feet as a result of the surface pressure formed between the seat and upper legs. Foot swelling may be caused by extended sitting, according to a study done by Winkel and Jorgensen. All of these issues are linked to the way pilots hold themselves when during flight.

The cockpit should be designed in such a way that it increases pilot comfort and efficiency. It should also enable the pilot to make regular minor postural adjustments without difficulty. The design of the pilot's seat, in particular, should encourage appropriate sitting posture and discourage bad habits.

During World War II, the United States performed the first study on pilot seat ergonomics. Pilots must sit for longer periods of time due to the increased range of flights. Previously, pilot seat design was dependent on subjective rating scales that were used to assess pilot comfort. Subjective feedback, on the other hand, was unable to significantly alter the pilot seat design, hence resolving pilot discomfort issues. As a result, the Air Force began incorporating objective measures as well as pilot feedback into seat design. Furthermore, there are only a few researches that have looked into objective measures using a pressure pad to analyze pressure distribution when seated. This approach proven to be a useful tool for evaluating pilot seat design.

Researchers frequently observe complex questionnaires, potential observer bias, misinformed rating systems and other issues when using subjective methods. Furthermore, objective methodologies fail to capture the pilot's view on seat design. As a result, both methodologies should be used to evaluate the pilot's seat. Nowadays, pilot seat design is evaluated using a variety of subjective discomfort scores as well as objective results such as temperature and humidity, posture, pressure distribution, vibration evaluation, spinal loading and so on. This allows designers to create a more comfortable seat for pilots flying longer flights.

For the evaluation of pilot seat design, various objective methodologies have evolved throughout time. Most studies, however, have placed a high value on the pressure distribution around the seat and the postural modifications made by pilots while flying the plane.

The civil aviation fleet had previously relied on military specifications for seat design. These criteria were developed by the military for practical functionality, not necessarily for comfort. According to Keegan et al. (1953), minimum standards for pilot chairs to ensure safety and comfort were introduced. These specifications are based on physiological, anatomical, and pathological reasons of lower back pain and discomfort.

However, the integration of a backrest and its adjustment at various angles is the first and most crucial necessity. Shoulder support, the angle between the trunk and the thigh, seat pan height, armrests, seat tilt adjustment to reduce kyphosis and seat pan curvature are among the other specifications in Keegan's model. With sufficient foot space to allow for posture changes based on Keegan's 11 seat design criteria, Harrison et al. (1999) proposed that fundamental pilot's seat design criteria include at least seat adjustability characteristics (seat inclination and height).

2.2 Advantage of new pilot seat cushion

Aviation seats generally have a long life and only involve maintenance issues, while seat cushions need to be replaced, usually every 3-4 years. With this market demand, there are also seat cushion designers and manufacturers.

The new innovative Octaspring® technology lies at the heart of the seat and backrest, giving 3-dimensional support by flawlessly adapting to pilot’s body, cradling it and offering first-class comfort.

Smart body zoning aids in the creation of ergonomically built seats that provide superior back support, allowing pilot’s spine to take on its natural shape, shoulders to relax, and circulation to enhance. The breathable Octaspring® springs may be made out of almost any foam density and stiffness level and they can be individually arranged to provide distinct support zones for different portions of the seat, which is given the largest amount of weight. This is the first totally zoned seat/sleep solution, providing targeted support for various body regions while boosting comfort and durability.

This cushion is up to 30% lighter because up to 50% less material is utilized in the manufacturing. Octaspring® technology produces fewer CO_2 emissions as well. Each seat cushion can save up to 150 grams of weight. This lowers transportation costs and fuel usage while also lowering CO_2 emissions, making it a very sustainable alternative.

The innovative air system naturally makes the seat cushion eight times more breathable without the use of wires or chemicals and it's been found to be 3°C cooler, which makes a big difference in providing cooler comfort for longer. The ventilation system ensures a steady flow of air – body movements push warm air out, damp air out of the cushion through specifically formed sides, allowing fresh air in. Independent comfort tests were carried out in order to evaluate the technology's comfort performance to that of excellent outcomes.

The cushions are made with foams that exceed certain industrial standards, including flame redundancy criteria, which are necessary in the aviation industry. The oil burner tests were performed with various combinations as well and prove fire resistible properties.

On three seat models, the Octaspring® seat cushion passed aviation standard fire redundancy testing (14 CFR/CS 25.853 (c), App.F to part II). After 80,000 cycles (with 750 N force), just 2.3% of the height was lost, with a return to the original height after a 24-hour recovery period. The Octaspring® seat cushion passed the 14G Dynamic Test with comparable results to regular seat cushions.

2.3 Calculation of the pilot's seat strength

For the airworthiness certification of the seat, it is important to meet the crash resistance performance requirements. For the crash resistance performance, the static test load can be increased to simulate the dynamic response test during a crash, that is, the seat and the tightening device must pass five thousand pounds. In the static load test 2000 pounds of force is allocated to the shoulder strap device and 3000 pounds of force is allocated to the waist belt device and the force acting direction is along the forward direction, as shown Fx^A and Fx^B in Fig. 2.1. Converted into international units $Fx^A = 8907$ N, $Fx^B = 13361$ N.

$$\theta_1 = \arctan\frac{101.62 - 88.82}{28.54} = 24.2,$$

$$\theta_2 = \frac{90 + \theta_1}{2} = \frac{90 - 24.2}{2} = 57.1.$$

The load Fx^A acting on the dummy A is balanced by the resultant force F_{11} of the safety shoulder belt and the force N_1 N_2 transmitted through the contact between the dummy A and the dummy B, as shown in the fig. 2.1 to establish a balance equation.

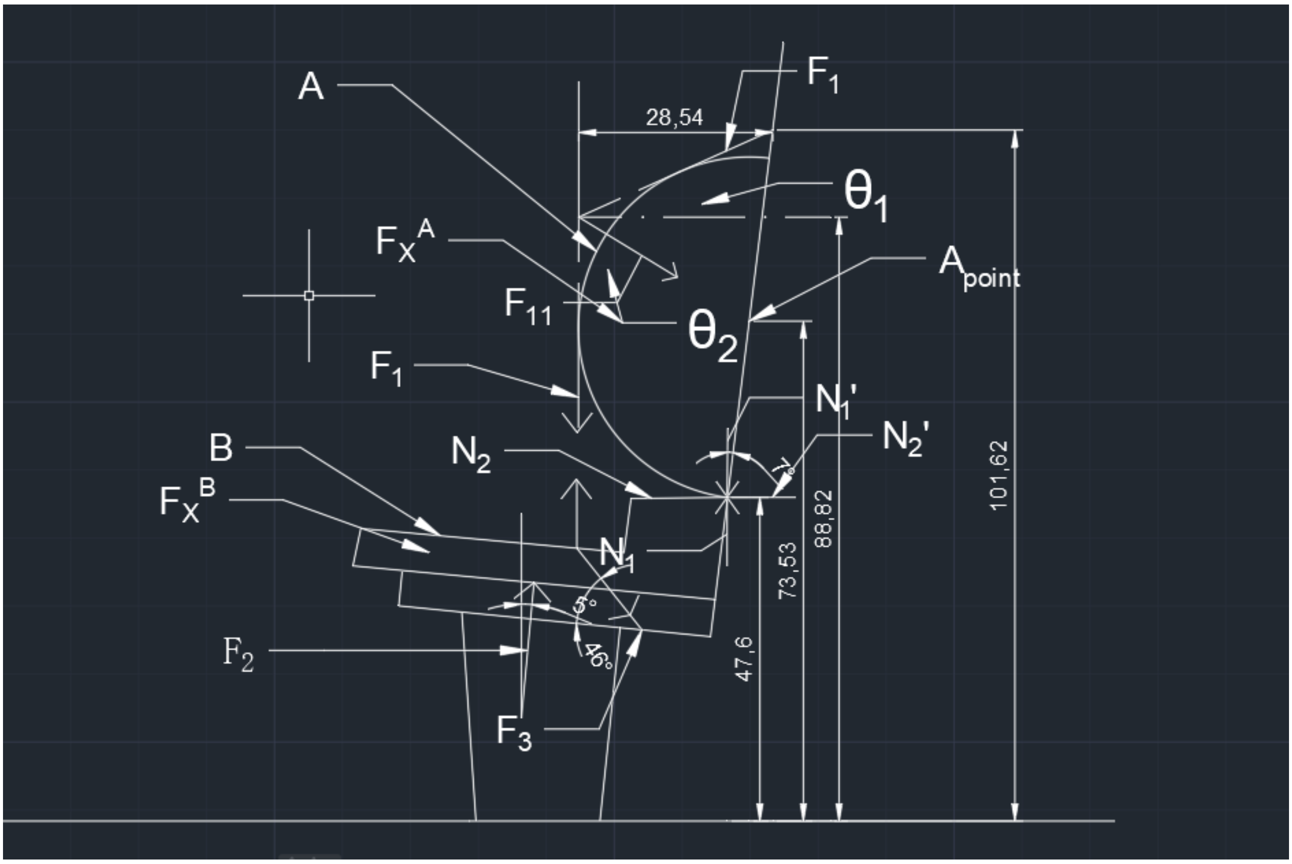

Fig. 2.1. Scheme of pilot's seat.

F_{11} – the force of the shoulder strap on the dummy A;

N_1 – the supporting force of dummy B to dummy A;

N_2 – friction force of dummy B to dummy A;

I_1N_1 – force arm to point A;

I_2N_2 – force arm to point A;

I_3F_{11} – force arm to point A;

F_1 – tensile force on the one direction of the shoulder strap;

$F_{shoulder}$ – tensile force on the one end of the shoulder strap;

F_2 – the supporting force of Chair surface to dummy B;

F_3 – tensile force on the one direction of the belt;

F_{belt} – tensile force on the one end of the belt;

N_1' – the overwhelming force of dummy B to dummy A;

N_2' – friction force of dummy A to dummy B.

According $\sum X = 0$ and $\sum Y = 0$:

$$Fx^A + N_2 = F_{11}\cos(\theta_2 - \theta_1)$$

$$N_1 = F_{11}\sin(\theta_2 - \theta_1)$$

Torque balance to A is:

$$N_1 \cdot I_1 + N_2 \cdot I_2 + F_{11} \cdot I_3 = 0,$$

So N_1 = 6258.5 N; N_2 = 763 N; F_{11} = 11590 N.

$$2F_1 \cdot \cos\theta_2 = F_{11} \to F_1 = 10688.7 \text{ N}.$$

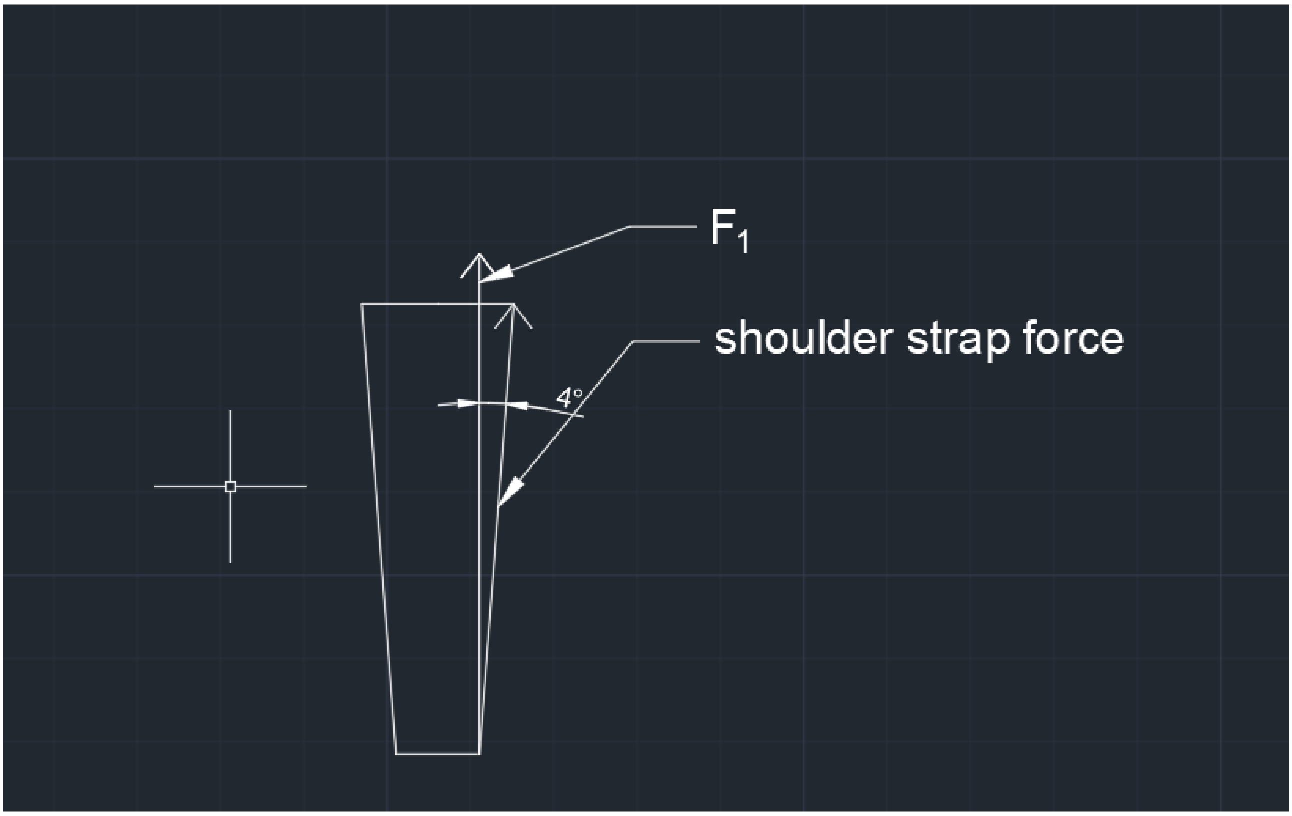

Fig. 2.2. Scheme of force calculation.

$$F_{shoulder} = \frac{F_1}{2 \cdot \cos\beta} = \frac{10688.7}{2 \cdot \cos 4} = 5347.4 \text{ N}.$$

The force acting on dummy B. In addition to the force Fx^B there are the load F_1 transmitted by the M-point shoulder belt through the seat belt, the force F_2 perpendicular to the seat surface and the load $N_1^{'}$ and $N_2^{'}$ transmitted by the dummy A through the O point.

According $\sum X = 0$ and $\sum Y = 0$:

$$N_2^{'} + Fx^B = F_3 \cdot \cos\theta_3 + F_2 \cdot \cos\theta_4$$

$$F_1 + F_2 \cdot \cos\theta_4 = F_3 \cdot \cos\theta_3 + N_1^{'}$$

As shown earlier $Fx^B = 13361$ N; $F_1 = 10688.7$ N; $N_1^{'} = 6258.5$ N; $N_2^{'} = 763$ N; $\theta_3 = 46°$; $\theta_4 = 5°$.

So $F_2 = 9831$ N; $F_3 = 19807.3$ N.

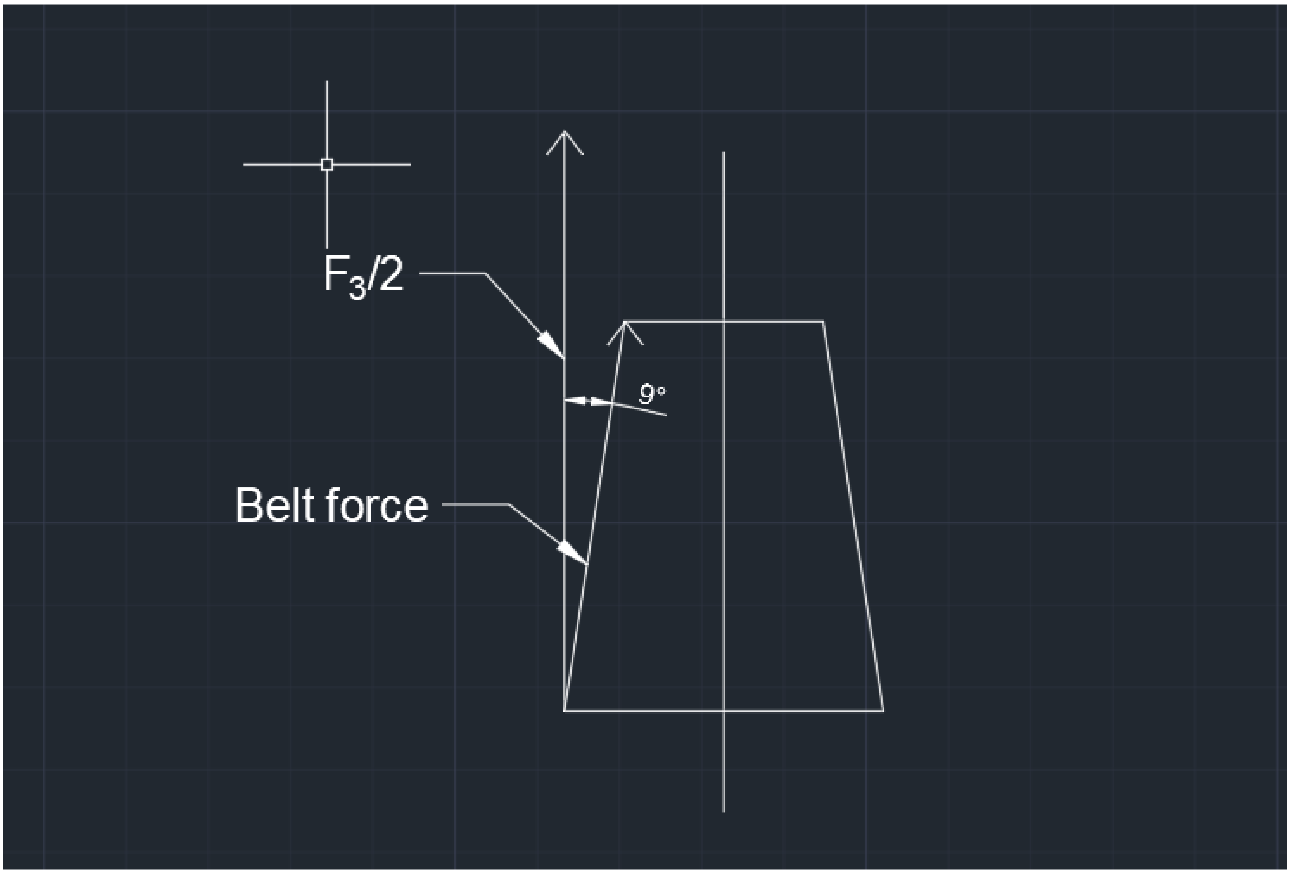

Fig. 2.3. Scheme of belt force calculation.

If $\alpha = 9°$

$$F_{belt} = \frac{F_3}{2 \cdot \cos\alpha} = 10027 \text{ N}.$$

Since the dummy, seat belt, and shoulder belt are in surface contact it is difficult to simulate accurately in the calculation and the force is extremely large. Therefore, the force analysis of the interaction between the components is used to obtain the experimental dummy acting on the seat. The forces acting on the parts, safety belts and shoulder belts were calculated. On this basis it is possible to choose a relatively safe seat belt.

Because for pilot's seat such a high meaning has a comfort, it was improved. The possibility of new technology to operate over time offers a consistent level of comfort throughout the life of the seat.

Conclusion to the special part

Flying for a long time, pilots often suffer from arthritis and cervical and lumbar diseases due to long-term sitting and lack of time for activity. Being on full alert in the cramped cockpit for a long time, mental fatigue can easily induce some diseases. So it is necessary to do everything we can to make the pilot feel at ease. Basic physical and clinical concepts should be considered when creating a seat cushion to ensure that the optimum decision is made. The seat cushion should be developed together with the pilot seat. This implies it isn’t necessary to give up all the goals at once (to the cushion or seat) and dimensional tweaks can be made to meet ergonomic and functional requirements.

It should be understood that choosing a seat cushion is not an easy task – no one cushion currently fits the needs of all users. The number of parameters that must be regulated is large and although a very structured approach was taken to cushion selection, one of two common difficulties can arise. The number of candidate cushions can be limited to a manageable quantity, resulting in compromises in the final product.

GENERAL CONCLUSIONS

The following are the outcomes of my design work:

- preliminary design of a middle-range aircraft with 150 passengers;
- cabin layout of a middle-range aircraft with 150 passengers;
- calculations of the airplane's center of gravity;
- calculations of the landing gear's key geometrical parameters;
- choice of wheels that meet the requirements.

Designed aircraft satisfies the planned aim of usage, its geometrical characteristics will provide the necessary aerodynamic performance, which will lead to efficient usage.

In the special part was improved the pilot’s seat cushion that provide:

- more comfort for pilot;
- less weight;
- better ergonomics;
- more safe and eco-friendly;
- meet all the aviation requirements and standards.

REFERENCE

1. Froom P. Low back pain in pilots / P. Froom, J. Barzllay, Y. Catne, S. Margaliot // Aviation Space and Environment Medicine. – No.57, 1986. – P. 694-695.
2. Lusted M. Evaluation of the seating of Qantas flight deck crew. / M. Lusted, S. Healey, and J.A. Mandryk // Ergonomics. – No.25, 1994. – P. 275-282.
3. Sharma S. Static anthropometry: Current practice to determine aircrew aircraft compatibility / S. Sharma, K.S. Raju, A. Agarwal // Indian Journal of Aerospace Medicine. – No.51, 2007. – P. 40-47.
4. Sallinen S. Sleep, alertness and alertness management among commercial airline pilots on short-haul and long-haul flights / S. Sallinen, M., Mikael, K. Ketola // Accident Analysis &Prevention. – No.98, 2017. – P. 320-329.
5. Cohen D. An objective measure of seat comfort / Aviation, Space, and Environmental Medicine. – No.69, 1998. – P. 410-414.
6. Wilson J.W.D. Background autonomic activity in medical students / J.W.D. Wilson, R.A. Dykman // Journal of Comparative and Physiological Psychology. – No.53, 1960. – P. 405-411.
7. Floyd W.F. Anatomical and Physiological Principles in a Chair and Table Design / W.F. Floyd, D.F. Roberts // Ergonomics. – No.2, 1958. – P. 1-16.
8. Winkel J. Evaluation of Foot Swelling And Lower Limb Temperatures in relation to Leg Activity during Long-Term Seated Office Work / J. Winkel, K. Jorgensen // Ergonomics. – No.29, 1986. – P. 313-319.
9. Looze D. Sitting comfort and discomfort and the relationships with objective measures / D. Looze, M.P. Kuij-Evers, L.F.M. Van Dieen // Ergonomics. – vol. 46, 2003. – P. 985-997.

10. Shen W. Validity and reliability of rating scales for seated pressure discomfort / W. Shen, K.C. Parsons // International Journal of Industrial Ergonomics. – No.20, 1997. – P. 441-461.

11. Eriksen C.A. Aircrew fatigue in trans-Atlantic morning and evening flights / C.A. Eriksen, T. Akerstedt // Chronobiology International. – No.23, 2006. – P. 843-858.

12. Keegan J.J. Alterations of the lumbar curve related to posture and seating / The Journal of Bone & Joint Surgery. – No.35, 1953. – P. 589-603.

13. Bongers P.M. Back pain and exposure to whole body vibration in helicopter pilots / P.M. Bongers, C.T.J. Hulshof, L. Dijkstra, H.C. Boshuizen, H.J.M. Groenhout, & E Valken // Ergonomics. – vol. 33, 1990. – P. 1007-1026.

Appendix

Appendix A

REQUEST FOR CALCULATION WORK

Student ………wanjiangnan………………………… Instructor ....

ADMITTED TO CALCULATION... (Data, Instructor's Signature)

МАКСИМАЛЬНОЕ ЧИСЛО ПАССАЖИРОВ **N** =....150...... ИЛИ МАКСИМАЛЬНАЯ МАССА ГРУЗА 19190**kg**;
Passenger Number or Maximum Payload

КОЭФФИЦИЕНТ ДОПОЛНИТЕЛЬНОЙ ЗАГРУЗКИ **К1**=...1.1.......; МАССА БЕЗПЛАТНОГО БАГАЖА **М.ББ** =20. **kg**;
Extra Load Factor Passenger Baggage

ЧИСЛО ЧЛЕНОВ ЭКИПАЖА **Ncrew** =.7......; РЕИСОВОЕ ВРЕМЯ ПОЛЕТА С МАС. ГРУЗОМ **Т** =.6.5...... **hours**;
Flight Crew Number Block Time with Maximum Payload

КОЛИЧЕСТВО БОРТПРОВОДНИКОВ **N** =...5....... ИЛИ СОПРОВОЖДАЮЩИХ **N** =............. ;
Attendant Number or Load Master Number

ОТНОСИТЕЛЬНАЯ МАССА МАКСИМАЛЬНОЙ КОММЕРЧЕСКОЙ НАГРУЗКИ 0.261.......;
Payload Fraction

ОТНОСИТЕЛЬНАЯ МАССА ТОПЛИВА ПРИ ПОЛЕТЕ С МАКСИМАЛЬНОЙ КОММЕРЧЕСКОЙ НАГРУЗКОЙ. 0.256.. ;
Fuel Fraction under Maximum Payload

ЭНЕРГОВООРУЖЕННОСТЬ САМОЛЕТА...........**kW/kg** ИЛИ ТЯГОВООРУЖЕННОСТЬ САМОЛЕТА.0.291**N/kg**;
Power-to-mass Ratio or Thrust-to-mass Ratio

КОЛИЧЕСТВО ОСНОВНЫХ ДВИГАТЕЛЕИ ....2..; КОЛИЧЕСТВО РЕВЕРСИРУЕМЫХ ДВИГАТЕЛЕЙ 2....... ;
Engine Number Engine Number Reversed

ДАЛЬНОСТЬ ПОЛЕТА С МАКСИМАЛЬНОЙ КОММЕРЧЕСКОЙ НАГРУЗКОЙ **L**=.5000.........**km**;
Flight Range with Maximum Payload

ВЫСОТА НАЧАЛА КРЕИСЕРСКОГО ПОЛЕТА ....11.27...**km**; КРЕИСЕРСКАЯ ЭКОНОМИЧЕСКАЯ СКОРОСТЬ 829 **km/h**;
Cruise Altitude Cruise Speed

СТРЕЛОВИДНОСТЬ КРЫЛА ПО 0.25 ХОРД В ГРАД.....28°..... ; СРЕДНЯЯ ОТН. ТОЛЩИНА КРЫЛА 12% (в долях);
Sweep Angle on One Quarter Line Mean Thickness Ratio (in fractions)

УДЛИНЕНИЕ КРЫЛА ПО ПОЛНОИ ПЛОЩАДИ ....9.39.........; СУЖЕНИЕ КРЫЛА ПО ПОЛНОЙ ПЛОЩАДИ.4.1 ;
Aspect ratio for Total Wing Area Taper Ratio for Total Wing Area

ТИП АЭРОДИНАМИЧЕСКОГО ПРОФИЛЯ КРЫЛА . .low wing........; ЗАКОНЦОВКИ "УИТКОМБА" yes (применяются или нет);
Airfoil Type Winglets (used or not)

ОТНОСИТЕЛЬНАЯ ПЛОЩАДЬ ПРИКОРНЕВЫХ НАПЛЫВОВ КРЫЛА (в долях).0.01 ...... ;
Relative Area of Wing Extensions (in fractions)

УСТАНОВЛЕНЫ НА КРЫЛЕ СПОЙЛЕРЫ ИЛИ ИНТЕЦЕРТОРЫ (да или нет) yes.......... ;
Spoilers used (yes or no)

МАКСИМАЛЬНЫЙ ЭКВИВАЛЕНТНЫЙ ДИАМЕТР ФЮЗЕЛЯЖА...3.7.........**m**; УДЛИНЕНИЕ ФЮЗЕЛЯЖА 9.51 ....;
Fuselage Maximum Equivalent Diameter Fuselage Fineness Ratio

СУММА УДЛИНЕНИЙ НОСОВОЙ И ХВОСТОВОЙ ЧАСТЕЙ ФЮЗЕЛЯЖА.2.1 .... ;
Sum of Fineness Ratios for Forward and Aft Fuselage Parts

МИНИМАЛЬНАЯ (**техническая**) ПОСАДОЧНАЯ СКОРОСТЬ **Vmin.** =…240 ....**km/h**;
Minimal Landing Speed

СТЕПЕНЬ МЕХАНИЗИРОВАННОСТИ КРЫЛА slats ...... (указать индексом по МУ);
High-lift Device Coefficient (index from Methodological Guide)

СТЕПЕНЬ ПОВЫШЕНИЯ ДАВЛЕНИЯ ДВИГАТЕЛЯ 31.3……..; СТЕПЕНЬ ДВУХКОНТУРНОСТИ ДВИГАТЕЛЯ 6.0;
Engine Pressure Ratio Engine By-pass Ratio

ДЛИНА ЛЕТНОЙ ПОЛОСЫ АЭРОДРОМА БАЗИРОВАНИЯ (ВПП + КПБ) 3.6............**km**;
Field Length Available (Runway + Stopway)

МАКСИМАЛЬНАЯ ВЫСОТА КРЕЙСЕРСКОГО ПОЛЕТА (практический потолок) **Hcr.max**. =12.5........... **km**;
Maximum Cruise Altitude (Flight Ceiling)

УГОЛ СТРЕЛОВИДНОСТИ ГОРИЗОНТАЛЬНОГО ОПЕРЕНИЯ В ГРАДУСАХ 29°..............;
Horizontal Tail Sweep Angle (in degrees)

УГОЛ СТРЕЛОВИДНОСТИ ВЕРТИКАЛЬНОГО ОПЕРЕНИЯ В ГРАДУСАХ 34°................ ;

Vertical Tail Sweep Angle (in degrees)

СУММА НЕУЧТЕННЫХ МАСС 50............**kg**. (*массы нетипичных систем и механизмов, дополнительные массы для оборудования салонов экстра класса, массы систем диагностики и встроенного контроля оборудования и основных систем самолета).*
Weights for Additional Equipment (equipment for high class passenger cabins)

INITIAL DATA AND SELECTED PARAMETERS

Passenger Number 150
Flight Crew Number 2
Flight Attendant or Load Master Number 5
Mass of Operational Items 1544.76
Payload Mass 15675.00

Cruising Speed 829
Cruising Mach Number 0.7784
Design Altitude 11.27
Flight Range with Maximum Payload 5000
Runway Length for the Base Aerodrome 3.30

Engine Number 2
Thrust-to-weight Ratio in N/kg 2.9100
Pressure Ratio 31.3
Assumed Bypass Ratio 5.5
Optimal Bypass Ratio 5.5
Fuel-to-weight Ratio 0.2560

Aspect Ratio 9.39
Taper Ratio 4.10
Mean Thickness Ratio 0.120
Wing Sweepback at Quarter Chord 28
High-lift Device Coefficient 1.05
Relative Area of Wing Extensions 0.01
Wing Airfoil Type
Winglets
Spoilers

Fuselage Diameter 3.70M
Finess Ratio 9.51

Horizontal Tail Sweep Angle 29.0
Vertical Tail Sweep Angle 34.0

CALCULATION RESULTS

Optimal Lift Coefficient in the Design Cruising Flight Point 0.46267

Induce Drag Coefficient 0.00913

ESTIMATION OF THE COEFFICIENT $D_m = M_{critical} - M_{cruise}$

Cruising Mach Number 0.77841
Wave Drag Mach Number 0.78904
Calculated Parameter D_m 0.01063
Wing Loading in kPa (for Gross Wing Area):
At Takeoff 4.987
At Middle of Cruising Flight 4.28
At the Beginning of Cruising Flight 4.800

Drag Coefficient of the Fuselage and Nacelles 0.00871
Drag Coefficient of the Wing and Tail Unit 0.00914

Drag Coefficient of the Airplane:
At the Beginning of Cruising Flight 0.02909
At Middle of Cruising Flight 0.02798
Mean Lift Coefficient for the Ceiling Flight 0.46267

Mean Lift-to-drag Ratio 16.53446

Landing Lift Coefficient 1.627
Landing Lift Coefficient (at Stall Speed) 2.440
Takeoff Lift Coefficient (at Stall Speed) 2.013
Lift-off Lift Coefficient 1.469
Thrust-to-weight Ratio at the Beginning of Cruising Flight 0.561
Start Thrust-to-weight Ratio for Cruising Flight 2.433
Start Thrust-to-weight Ratio for Safe Takeoff 2.349

Design Thrust-to-weight Ratio 2.531

Ratio $D_r = R_{cruise} / R_{takeoff}$ 1.036

SPECIFIC FUEL CONSUMPTIONS (in kg/kN*h):
Takeoff 36.5630
Cruising Flight 57.2486
Mean cruising for Given Range 58.8472

FUEL WEIGHT FRACTIONS:
Fuel Reserve 0.03203
Block Fuel 0.22634

WEIGHT FRACTIONS FOR PRINCIPAL ITEMS:
Wing 0.11492
Horizontal Tail 0.01112
Vertical Tail 0.01097
Landing Gear 0.04011
Power Plant 0.08142
Fuselage 0.09735
Equipment and Flight Control 0.13412
Additional Equipment 0.01203
Operational Items 0.02149
Fuel 0.25837
Payload 0.21803

Airplane Takeoff Weight 71894

Takeoff Thrust Required of the Engine 90.97

Air Conditioning and Anti-icing Equipment Weight Fraction 0.0230
Passenger Equipment Weight Fraction 0.0169
(or Cargo Cabin Equipment)
Interior Panels and Thermal/Acoustic Blanketing Weight Fraction 0.0073
Furnishing Equipment Weight Fraction 0.0123
Flight Control Weight Fraction 0.0065
Hydraulic System Weight Fraction 0.0176
Electrical Equipment Weight Fraction 0.0327
Radar Weight Fraction 0.0032
Navigation Equipment Weight Fraction 0.0048
Radio Communication Equipment Weight Fraction 0.0024
Instrument Equipment Weight Fraction 0.0056
Fuel System Weight Fraction 0.0075

Additional Equipment:
Equipment for Container Loading 0.0083
No typical Equipment Weight Fraction

(Build-in Test Equipment for Fault Diagnosis, 0.0037
Additional Equipment of Passenger Cabin)

TAKEOFF DISTANCE PARAMETERS

Airplane Lift-off Speed 265.16
Acceleration during Takeoff Run 1.83
Airplane Takeoff Run Distance 1479
Airborne Takeoff Distance 578
Takeoff Distance 2058

CONTINUED TAKEOFF DISTANCE PARAMETERS

Decision Speed 251.91
Mean Acceleration for Continued Takeoff on Wet Runway 0.09
Takeoff Run Distance for Continued Takeoff on Wet Runway 4411.45
Continued Takeoff Distance 4989.83m
Runway Length Required for Rejected Takeoff 5176.00m

LANDING DISTANCE PARAMETERS

Airplane Maximum Landing Weight 58266
Time for Descent from Flight Level till Aerodrome Traffic Circuit Flight 22
Descent Distance 50.68
Approach Speed 243.97
Mean Vertical Speed 1.98
Airborne Landing Distance 515
Landing Speed 228.97
Landing run distance 729
Landing Distance 1243
Runway Length Required for Regular Aerodrome 2076
Runway Length Required for Alternate Aerodrome 1165